Microscopic origin of the Dynes parameter Γ of the LaAlO₃–SrTiO₃ interface superconductor

Hans Boschker,[1,*] Evangelos Fillis-Tsirakis,[1] Christoph Richter,[1,2] Ding Zhang,[1,†] Jurgen Smet,[1] and Lukas Kuerten [1,3]

[1]*Max Planck Institute for Solid State Research, 70659, Stuttgart, Germany*
[2]*Center for Electronic Correlations and Magnetism, Augsburg University, 86135, Augsburg, Germany*
[3]*Department of Materials, ETH Zurich, 8093, Zurich, Switzerland*

The superconducting density of states of the two-dimensional electron system at the LaAlO₃–SrTiO₃ interface exhibits broad quasiparticle peaks that are well described by the Dynes parameter Γ. We measured Γ in a wide range of temperatures and gate voltages using tunneling spectroscopy. Γ exhibits a T^q temperature dependence, with $q = 2.2 \pm 0.2$. We discuss several interpretations of Γ and conclude that Γ is an intrinsic parameter of the superconducting state that quantifies the effect of the pair-breaking processes in the superconductor. The strong temperature dependence at low temperatures rules out inelastic electron scattering and magnetic scattering as the origin of the pair breaking. We find that Γ can be explained by interband scattering and by scattering in a superconductor with nodes in the order parameter.

I. INTRODUCTION

The Bardeen-Cooper-Schrieffer (BCS) theory of superconductivity is one of the cornerstones of condensed-matter physics [1]. The theory correctly predicts that superconductors are characterized by the appearance of a gap Δ in the electron density of states below the critical temperature T_c. The magnitude of the gap scales with T_c and the spectral weight accumulates in sharp quasiparticle peaks bordering the gap. These quasiparticle peaks in the density of states are broader than the expectation of the BCS theory in several superconductors. Dynes *et al.* attributed this broadening to the finite lifetime of the quasiparticle states by inserting a phenomenological parameter Γ in the equation for the density of states N:

$$N(E) = \mathrm{Re}\left[\frac{E - i\Gamma}{\sqrt{(E - i\Gamma)^2 - \Delta^2}}\right], \qquad (1)$$

where E is the energy [2]. Next to broadening of the quasiparticle peaks, Eq. (1) also predicts $N(E)$ to be nonzero for all energies when $\Gamma > 0$. Several authors have criticized this description on the basis that the parameter is not directly derived from a microscopic pair-breaking mechanism [3,4]. Nevertheless, the excellent match between the

experimentally observed density of states in a range of superconductors [2,5–8] and Eq. (1) poses several questions. Why does a single parameter Γ describe the experiments so well and which fundamental physics does Γ represent?

Furthermore, several superconductors exist in which the resistive T_c differs from the temperature at which the gap opens [9–13]. This anomaly occurs often in two-dimensional superconductors with low charge-carrier densities n. A prominent example is the electron system generated at the interface between LaAlO₃ and SrTiO₃ [14,15]. This two-dimensional superconductor can be tuned through a superconducting dome by electrostatic gating [16]. On the underdoped side of the dome, T_c decreases with decreasing n. However, Δ and the temperature at which the gap closes, T_{gap}, increase with decreasing n (Ref. [12]). The tunnel spectra below as well as above T_c are well described by Eq. (1). Because both $\Delta(T)$ and $\Gamma(T)$ are of similar magnitude and are smoothly varying with T for $T \approx T_c$, it is not clear which parameter controls T_c. It was found, however, that the Δ_0/Γ_0 ratio predicts T_c surprisingly well [12]. Here, Δ_0 (Γ_0) is Δ (Γ) at $T = 0$ K. This indicates that Γ plays a role in setting T_c in this superconductor.

The influence of Γ on T_c has also been observed in granular Al samples [17] and is consistent with the broadened superconducting gaps observed in insulating samples of amorphous InO and TiN [18–20]. Several experiments link Γ to T_c in underdoped cuprates as well [21–24]. Finally, the superconducting gap in the lithium-intercalated layered nitrides Li$_x$HfNCl and Li$_x$ZrNCl is present above T_c, similar to underdoped LaAlO₃–SrTiO₃ and Γ is of similar magnitude as Δ for $T_c < T < T_{gap}$ (Ref. [13]). The importance of Γ in setting T_c, however, is not a general property of superconducting materials. For example, the T_c of MoC films depends strongly on the film thickness and Γ increases from 0 to 0.85 Δ with decreasing film thickness. Nevertheless, T_c is solely governed by Δ_0 for all these MoC films [8,25].

*h.boschker@fkf.mpg.de
†Present address: State Key Laboratory of Low-Dimensional Quantum Physics and Department of Physics, Tsinghua University, Beijing, 100084, China.

Here, we analyze the tunnel spectra of the $LaAlO_3$–$SrTiO_3$ two-dimensional superconductor in order to systematically investigate the behavior of Γ in the superconducting dome and to determine the origin of Γ. We find that Eq. (1) describes the tunnel spectra extremely well. The strong temperature dependence of Γ at low temperatures rules out inelastic electron scattering and magnetic scattering as the origin of the pair breaking. We find that a multiband model with both superconducting and nonsuperconducting bands can lead to tunnel spectra identical to Eq. (1) and that this is a possible origin of the pair breaking in the $LaAlO_3$–$SrTiO_3$ interface superconductor. Furthermore, the origin of Γ can also be scattering in a superconductor with an order parameter with nodes in the gap structure.

II. EXPERIMENT

The tunnel junctions comprise the electron system of the $LaAlO_3$–$SrTiO_3$ heterostructure as one electrode, the 1.6-nm-thick $LaAlO_3$ layer as the insulator and a Au counterelectrode. Using pulsed laser deposition, monitored by reflection high-energy electron diffraction, $LaAlO_3$ films were grown onto TiO_2-terminated $SrTiO_3$ substrates (CrysTec GmbH) at an oxygen pressure of $1 - 2 \times 10^{-4}$ mbar at $780\,°C$–$800\,°C$. The $LaAlO_3$ was ablated from a single-crystalline target with a laser fluence of $1\,J/cm^2$. After annealing, 30 nm of Au were deposited onto the sample surfaces either by pulsed laser deposition or by radio-frequency sputtering after an *in situ* transfer into a sputtering system. Subsequently, the Au was patterned into photolithographically defined, ring-shaped electrodes using a $KI+I_2$ etch solution. The electrode areas range from 0.2 to 1 mm^2. Contacts to the 2DEL were made by refilling Ar-ion-etched pits with sputtered Ti and Au. We attached wires to the top electrode using Ag glue and to the contacts to the 2DEL by wedge bonding. More detailed information about the junctions and their characteristics is found elsewhere [12,26–29].

We measured tunneling characteristics by sourcing current from the top electrodes to outer contacts on the electron system and measuring the voltage between the top electrodes and the electron system with a separate set of contacts. We used dc current bias together with a small ac current to directly measure $V(I)$ and $dV/dI(I)$. The measurements were performed in a top-loading-into-mixture dilution refrigerator with a base temperature of 20 mK. This is significantly colder than our previously reported measurements [12] which were performed in a cold finger dilution refrigerator with a base temperature of 50 mK. We took special care to avoid broadening of spectral features by electrical noise from the environment. The lower electron temperature during the measurements allows for a precise determination of the intrinsic broadening of the superconducting quasiparticle peaks. To tune the superconducting state electrostatically, a gate voltage V_G was applied to the Ag-coated back side of the $SrTiO_3$ substrate while the electron system was held at ground potential. We measured magnetotransport in the van der Pauw configuration in a Quantum Design Physical Properties Measurement System at $2 < T < 300$ K in order to extract the temperature dependence of the normal-state scattering rate of the electron system.
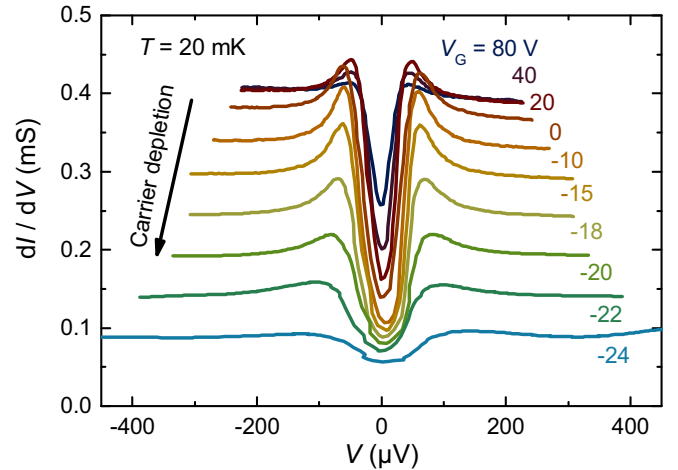

FIG. 1. Tunnel spectra of device A for different V_G measured at $T = 20$ mK. For $V_G < 20$ V, the normal-state conductance of the junction decreases with decreasing V_G. For $V_G < -25$ V, the device is insulating. The superconducting gap is present for all V_G and increases with decreasing n. Significant broadening of the quasiparticle peaks is observed. This broadening increases with decreasing n.

III. RESULTS

Figure 1 presents the gate voltage (V_G) dependence of the tunneling spectra of one of the devices on sample A at $T = 20$ mK. Superconducting gaps are observed in all spectra. For $V_G > 0$ V, the normal-state conductance is independent of V_G whereas the superconducting gap becomes smaller with increasing n. For $V_G < 10$ V, the normal-state conductance decreases with decreasing n. The superconducting gap remains present in all spectra. For $V_G < -25$ V, the device was insulating and no measurements could be performed. The data agree well with the data published before [12,26]. In particular, the superconducting gap persists when the device is turned insulating, the superconducting gap decreases in size with increasing n, and the increase of the normal-state conductance with increasing n saturates, indicating a Lifshitz transition of the electron system. For all V_G, significant tunnel conductance is present at zero bias ($V = 0\,\mu V$), indicating the importance of Γ in describing the spectra.

In order to extract Δ and Γ from the tunneling data, we fitted the data with the quasiparticle-lifetime-broadened density of states convoluted with the derivative of the Fermi function. Reliable fits are obtained once the measured energy dependence of the density of states in the normal state is taken into account. Figure 2 illustrates the data-analysis procedure. The shape of the normal-state conductance is measured at $T > T_c$ and used as a background for the fits at $T < T_c$. The normal-state conductance is not constant as a function of V. First, the normal-state conductance increases with increasing voltage, reflecting the increase of the density of states with energy in the electron system. Second, a small depression around zero voltage is present. This is attributed to an Altshuler-Aronov correction [30] to the density of states of a disordered electron system. This correlation gap becomes more pronounced with decreasing n. Once these features are taken into account, excellent fits between the model and the experiment are obtained
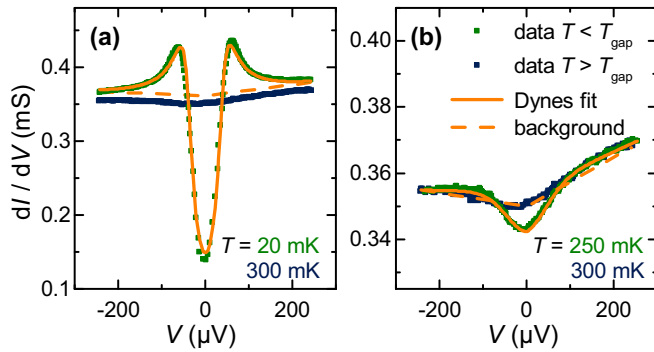
FIG. 2. Tunnel spectra above (blue symbols) and below (green symbols) $T_{gap} = 270$ mK for $V_G = 0$ V. The graphs illustrate the data analysis procedure. The shape of the tunnel spectrum for $T > T_{gap}$ is used as a background normal-state conductance. This background conductance is modified by the presence of the superconducting gap. The fits for the gap are based on Eq. (1) and the thermal distribution of the electrons in the Au counterelectrode. Excellent fits are obtained, both at $T = 20$ mK (a) and at $T = 250$ mK, which is close to T_{gap} (b).

(see Fig. 2). We note that when the Altshuler-Aronov correction is not taken into account, the data do not seem to preserve spectral weight when the superconducting gap opens. Therefore, reference spectra of the normal-state density of states are required for a reliable extraction of the superconducting parameters.

The gate voltage dependence of Δ and Γ are shown in Fig. 3(a) for $T = 20$ mK. Δ increases monotonically from 20 to 60 μeV with decreasing V_G. In contrast, Γ is almost constant at ~ 18 μeV for $V_G > -10$ V, but rapidly increases up to 60 μeV with decreasing V_G for $V_G < -10$ V. The gate-voltage dependence of the ratio Δ/Γ ($T = 20$ mK) is shown in Fig. 3(b). The ratio has a maximum of 3 at $V_G = -10$ V. Based on previous measurements we expect this maximum to correspond to the maximum of T_c [12]. (T_c was not directly measured in this device.) Another indication for the maximum of T_c is the saturation of the normal-state resistance of the tunnel junction that indicates the Lifshitz transition in the electron system [26]. This happens at $V_G = 10$ V in this device. This Lifshitz transition occurs at the maximum of the super-

conducting dome of the LaAlO$_3$–SrTiO$_3$ superconductor in a number of studies [26,31,32]. Therefore, and because the device is insulating for $V_G < -25$ V, the range of V_G shown in Fig. 3 encompasses most of the superconducting dome.

Figure 4 presents the temperature dependence of the tunnel spectra for six values of V_G. In all spectra, significant tunnel conductance is present at $V = 0$ μV. Furthermore, the conductance at $V = 0$ μV increases with increasing temperature because spectral weight is transferred from the quasiparticle peaks to the gap. These observations highlight the importance of Γ in describing the tunnel spectra. The temperature dependence of Δ and Γ is shown in Fig. 5. $\Delta(T)$ closely follows the temperature dependence expected from the BCS theory for all gate voltages. Γ increases rapidly with increasing temperature and is typically larger than Δ for $T > 0.5 T_{gap}$. We fitted the temperature dependence of Γ to the function $\Gamma(T) = \Gamma_0 + \Gamma_1 T^q$. This function describes the data well, except for the data at $V_G = 80$ V. We find q to be 2.2 ± 0.2.

In order to search for a possible link between the temperature-dependent and the temperature-independent contributions to Γ, we repeated the fits under the constraint of $q = 2.2$. The result is shown in Fig. 6. There is a positive correlation between the parameters such that $\Gamma(T) \approx \Gamma_0(1 + 1.4 \times 10^{-5} \ T^{2.2})$. This correlation suggests that the two contributions have a common origin.

IV. DISCUSSION

A. Necessity of Γ in describing the superconductor

We first review the arguments to analyze the broadening of the quasiparticle peaks in the tunnel spectra as an intrinsic feature of the superconducting density of states. Several extrinsic sources of broadened quasiparticle peaks in tunnel spectra exist. First of all, the quasiparticle peaks are naturally broadened as a result of the convolution with the derivative of the Fermi function due to thermal excitations in the metal counter electrode. This process is taken into account in the data analysis, but could result in errors if the measurement temperature is higher than expected. The error in T in our experiment is smaller than 5 mK, however, as determined by the observation of fragile quantum Hall states in this measurement setup [33]. This error is much smaller than the values required to explain the large broadening of the quasiparticle peaks. Furthermore, it would be inconsistent with the dependence of the broadening on both T and V_G. These dependencies also rule out environment-assisted tunneling [34] as the origin of the spectral broadening.

Another source of broadening is the probability function $P(E)$. It describes the energy-resolution function of tunnel junctions due to the charging energy imposed by the quantized nature of the electron charge [35]. This process is not relevant for our experiment because it applies only in the limit of junctions with a small capacitance, e.g., a scanning-tunneling-microscopy experiment. Our junctions have a capacitance of ~ 50 nF, resulting in an intrinsic energy resolution of 0.01 μeV, which is much smaller than the thermal resolution.

Finally, the observed broadening could also be due to spatial inhomogeneities in the electron system. To analyze this scenario, we model a typical superconducting density of states
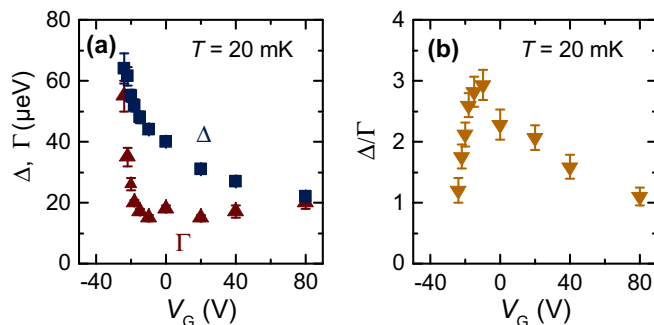

FIG. 3. (a) The gate-voltage dependence of Δ and Γ extracted from the data shown in Fig. 1. (b) The ratio Δ/Γ has a maximum at $V_G = -10$ V. Positive values of V_G correspond to enhancement of n. The data were measured at $T = 20$ mK.
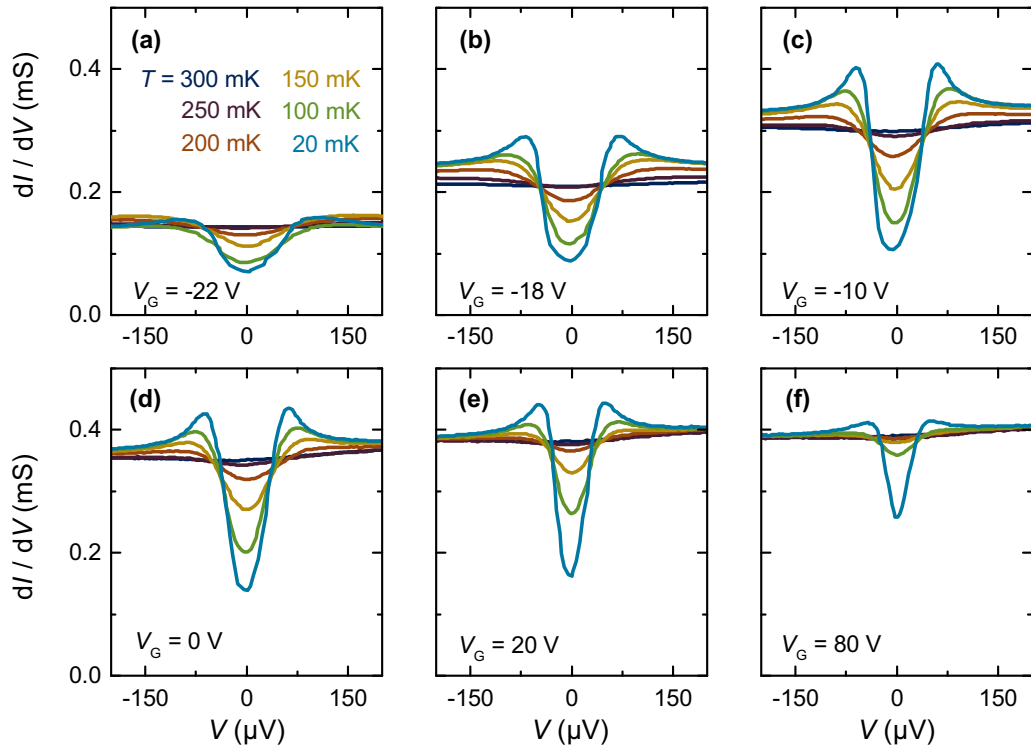
FIG. 4. Temperature dependence of the tunnel spectra for six values of V_G. In all spectra, significant broadening of the quasiparticle peaks is observed. This highlights the importance of Γ in describing the tunnel spectra. The temperature at which the gap closes, T_{gap}, increases with increasing Δ_0.

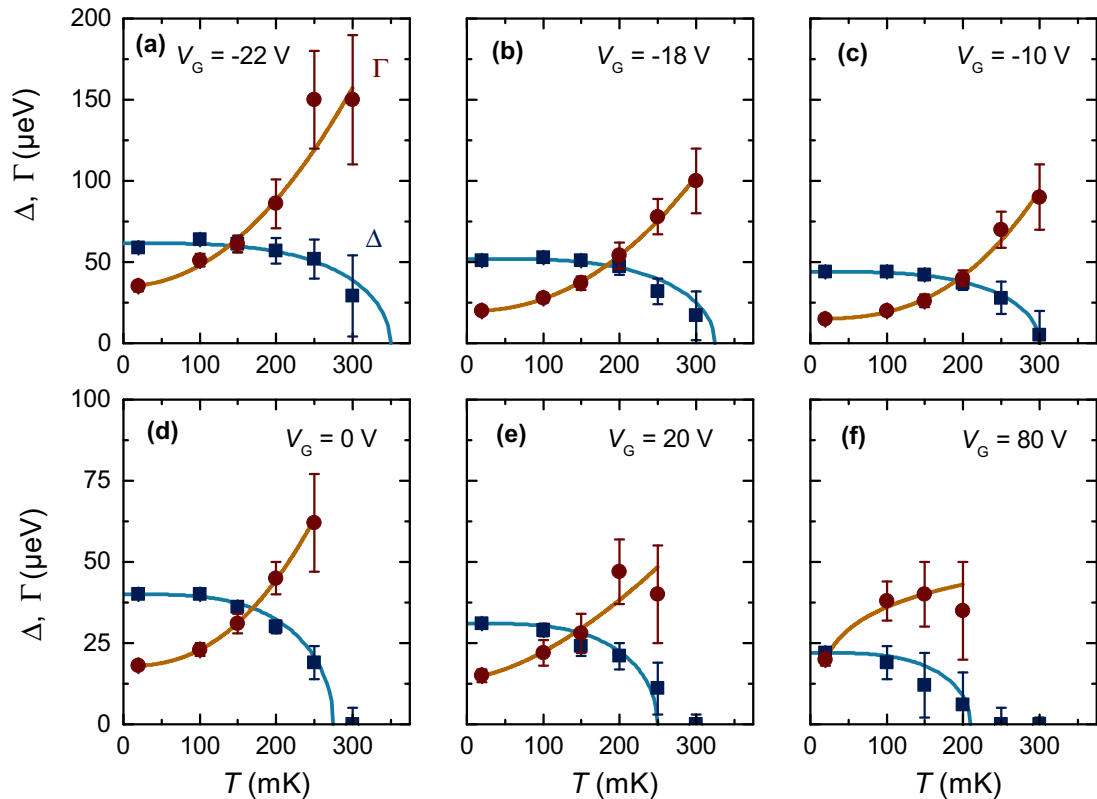FIG. 5. Temperature dependence of Δ and Γ extracted from the data shown in Fig. 4. Δ decreases with increasing temperature following the BCS prediction (blue solid lines). Γ increases with increasing temperature and is typically larger than Δ for $T > 0.5 T_{gap}$. The orange solid lines are fits to $\Gamma(T) = \Gamma_0 + \Gamma_1 T^q$. Error bars define the 90% confidence interval.
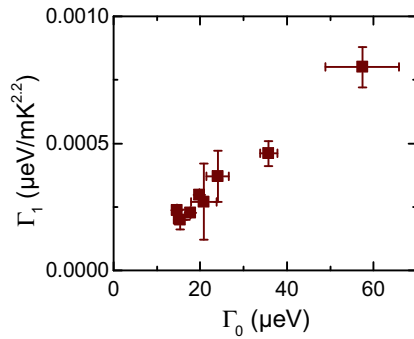
FIG. 6. Correlation between the temperature-independent (Γ_0) and the temperature-dependent (Γ_1) contributions to Γ. This graph contains data points for $V_G = -24, -22, -20, -18, -10, 0, 20$ and 80 V. A positive correlation is observed between both parameters.

$N(E)$ with $\Delta = 40$ μeV and $\Gamma = 15$ μeV [see Fig. 7(a)]. In order to describe the spectrum without intrinsic broadening, we allow for areas of the device to have a variation in Δ. As shown in Fig. 7, this $N(E)$ is perfectly described by a system in which $\sim$35% of the device area is not superconducting and the remaining area is superconducting with a Lorentzian distribution of Δ centered around 40 μeV with a width of 30 μeV (2Γ). We note that this distribution is uniquely defined by the values of Δ and Γ. This gap distribution will have the usual BCS temperature dependence with $2\Delta = 3.5k_B T_{gap}$ for each individual region of the gap. The resulting temperature dependence of the system is shown in Fig. 7(b). The gap fills in with increasing temperature, but at a lower rate than that of a superconducting system with a single gap. A gap remains in $N(E)$ up to temperatures twice the T_{gap} that corresponds to a gap of 40 μeV. Figure 7(c) shows the extracted $\Delta(T)$ and $\Gamma(T)$ by analyzing the temperature dependence of the gap distribution with a single gap. $\Delta(T)$ deviates significantly from the BCS expectation, in contrast to the $\Delta(T)$ extracted from the measurements as shown in Fig. 5.
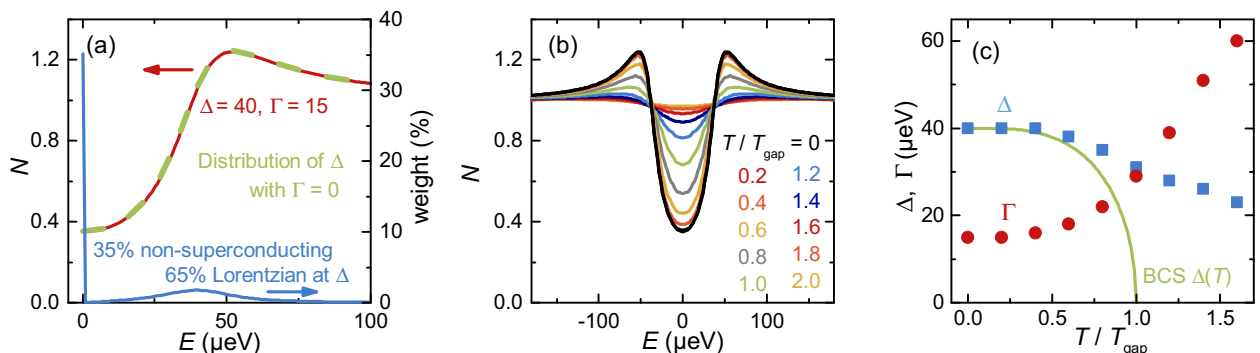
This discrepancy demonstrates that this model of spatially inhomogeneous superconductivity is inconsistent with the data. We conclude that the broadening of the quasiparticle peaks in the tunnel spectra is intrinsic.

All measured tunnel spectra are well described by Eq. (1), as shown in Fig. 2. In contrast, other models describing quasiparticle-peak broadening such as models based on exchange scattering by paramagnetic impurities [36], mesoscopic conductance fluctuations [37], or short-range superconducting fluctuations [4] do not describe the data well. These alternative models either predict a full gap at small energies or a reduction of spectral weight in the quasiparticle peaks. These predictions are not observed. Therefore, we conclude that the Dynes parameter Γ is a necessary ingredient for the correct description of the shape of $N(E)$ in superconducting LaAlO$_3$–SrTiO$_3$.

B. Microscopic interpretation of Γ

The broadening of the quasiparticle peaks in $N(E)$ is due to pair-breaking scattering because pair-breaking scattering limits the lifetime of the quasiparticle states. Several mechanisms for pair breaking exist and we discuss these in turn below.

1. Inelastic electron scattering

The standard explanation for the Dynes spectrum is that it is caused by inelastic electron-phonon scattering [38,39]. Because inelastic scattering is also the cause of electrical resistivity in normal-metal transport, it is instrumental to compare the Dynes scattering rate Γ with the normal-state scattering rate Γ_N. Figure 8 shows the temperature-dependent values of Γ obtained from three different LaAlO$_3$–SrTiO$_3$ samples together with the temperature-dependent values of Γ_N for both lightly and heavily doped SrTiO$_3$ (Ref. [40]) and LaAlO$_3$–SrTiO$_3$. The Γ_N data of LaAlO$_3$–SrTiO$_3$ were obtained from magnetotransport measurements. The figure also shows the spin-scattering rate Γ_S of LaAlO$_3$–SrTiO$_3$ [41]. $\Gamma(T)$ is relatively small, but has strong temperature

FIG. 7. Simulated $N(E)$ for a model with a distribution of Δ and with $\Gamma = 0$. (a) The $N(E)$ corresponding to a superconductor with $\Delta = 40$ μeV and $\Gamma = 15$ μeV can be reproduced by a model in which 35% of the area is nonsuperconducting, and 65% of the area is superconducting with a Lorentzian distribution of Δ centered around 40 μeV with a width of 30 μeV. The blue line shows the distribution of the model with the gap energy Δ on the x axis. The nonsuperconducting part is plotted at $\Delta = 0$ μeV. (b) Temperature dependence of $N(E)$ of the model with the Δ distribution assuming an independent BCS temperature dependence for all values of Δ. A gap structure persists in $N(E)$ at temperatures far above the T_{gap} corresponding to $\Delta = 40$ μeV because gap values larger than 40 μeV are present in the distribution. (c) The result of extracting a single Δ and Γ value from the $N(E)$ shown in (b). This $\Delta(T)$ does not follow the BCS prediction, in contrast to the experimental data in Fig. 5.
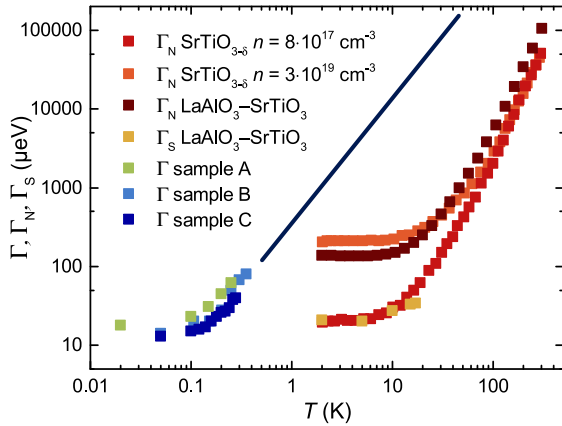
FIG. 8. Comparison between the Dynes scattering rate Γ, the normal-state scattering rate Γ_N, and the spin-scattering rate Γ_S. The data for doped SrTiO$_3$ were taken from Ref. [40] and the data for Γ_S were taken from Ref. [41]. Extrapolating the temperature dependence of Γ toward high temperatures leads to values of scattering rates larger than the observed rates of Γ_N and Γ_S. This indicates that the mechanisms that cause Γ_N and Γ_S are not the mechanism that causes Γ.

dependence for $T < 0.5$ K. In contrast, $\Gamma_N(T)$ is relatively large and is temperature independent for $T < 10$ K.

Inelastic scattering can only be the main cause of the pair-breaking scattering if the normal-state scattering rate is larger than the pair-breaking scattering rate [42] The low-temperature values of Γ_N of lightly doped SrTiO$_3$ are of similar magnitude as the Γ values and all other values of Γ_N are larger. The strong temperature dependence of Γ, however, is inconsistent with an interpretation of inelastic scattering as the origin of Γ. In electronic systems whose bandwidth is larger than the temperature, scattering rates do not saturate with increasing temperature. Therefore, $\Gamma(T)$ can be extrapolated toward the temperature range in which $\Gamma_N(T)$ was measured (see Fig. 8). For $T > 10$ K, we find that the extrapolated scattering rate is several orders of magnitude larger than Γ_N. So, if Γ was caused by an inelastic scattering process, this process would dominate the resistivity of the LaAlO$_3$–SrTiO$_3$ electron system at $T > 10$ K, and the electron system would have a much higher resistivity than the measured resistivity. Therefore, Γ is not caused by either inelastic electron-phonon scattering or inelastic electron-electron scattering.

2. Magnetic scattering

Magnetic scattering breaks Cooper pairs, but does not easily bring about the $N(E)$ described by Eq. (1) (Ref. [36]). Magnetic impurities typically lead to the formation of Yu-Shiba-Rusinov states [43–45]. Recently, it was shown, however, that a Lorentzian distribution of a large number of magnetic scatterers does result in the Dynes $N(E)$ [46–49]. Magnetic effects can be present at the LaAlO$_3$–SrTiO$_3$ interface (see Ref. [50] and references therein), but the spin-scattering rate is low. The experimentally measured spin lifetime is ~150 ps and it has a weak temperature dependence for $2 < T < 15$ K [41,51]. This corresponds to spin-scattering rates Γ_S of 20 to 35 μeV (see Fig. 8). $\Gamma_S(T)$ is of similar

magnitude as $\Gamma(0)$, but smaller than the Γ values around $T \approx T_{gap}$, even though the values for Γ_S were measured at higher temperatures than the values for Γ. The strong temperature dependence of Γ is also not consistent with the weak temperature dependence of Γ_S. This comparison shows that the two scattering rates do not correspond to the same physical process. Therefore, we exclude magnetic scattering as the origin of Γ in the LaAlO$_3$–SrTiO$_3$ interface superconductor.

3. Unconventional order-parameter symmetry

Several superconductors have an unconventional order-parameter symmetry with a gap function that depends on the direction of momentum. In these superconductors, elastic scattering is pair breaking because the scattering changes the direction of momentum of the charge carriers and the gap function is typically different before and after the scattering event. The standard example is the scattering in d-wave superconductors such as the cuprates. The gap symmetry of LaAlO$_3$–SrTiO$_3$ interface superconductor has not been determined yet. There are several arguments that the LaAlO$_3$–SrTiO$_3$ interface superconductor has s-wave symmetry. First, doped SrTiO$_3$ is known to be an s-wave superconductor [52,53]. The critical temperatures of doped SrTiO$_3$ and LaAlO$_3$–SrTiO$_3$ are very close, suggesting that the pairing mechanism and therefore also the order-parameter symmetry are the same. Furthermore, the presence of nodes in the order parameter changes the shape of $N(E)$ in the superconductor. Based on the analysis of numerous measured tunnel spectra, we find the nodeless component of the order parameter in LaAlO$_3$–SrTiO$_3$ to be larger than 90% in the tunneling direction. For example, the quality of the fits shown in Fig. 2 would not be possible with a model of a nodal superconductor. But, several other experiments suggest a more complex order-parameter symmetry to be present in this or similar superconducting heterostructures [54–57]. Furthermore, the relation between the superconducting condensate and the Rashba spin-orbit coupling [58] of the electron system has not yet been resolved. Therefore, pair-breaking scattering due to a more complex order-parameter symmetry cannot be excluded and is a possible origin of the pair breaking. This scenario requires the complex order parameter to have nodes in the gap structure.

4. Interband scattering

Interband scattering is a pair-breaking mechanism when the gaps in both bands differ. But, interband scattering also causes the gaps in both bands to equalize [59]. This is why doped SrTiO$_3$ is a multiband superconductor with a single gap [60]. The question is then whether a situation arises in which interband scattering is sufficiently strong to induce pair breaking in the entire energy range without equalizing the gaps in both bands. We therefore look at the equations describing a coupled two-band superconducting system [59,61,62]:

$$\Delta_1(E) = \Delta_1^{BCS} - \Gamma_{12} \frac{\Delta_1(E) - \Delta_2(E)}{\sqrt{\Delta_2^2(E) - E^2}},$$

$$\Delta_2(E) = \Delta_2^{BCS} - \Gamma_{21} \frac{\Delta_2(E) - \Delta_1(E)}{\sqrt{\Delta_1^2(E) - E^2}}. \tag{2}$$

Here, $\Delta_{1,2}^{\mathrm{BCS}}$ are the bare order parameters for the first and second band, respectively, and Γ_{12} and Γ_{21} are the coupling parameters between the bands. The coupling parameters are proportional to the density of states $N_{1,2}$ at the Fermi level in the bands in the following way:

$$\frac{\Gamma_{21}}{\Gamma_{12}} = \frac{N_1(E_{\mathrm{F}})}{N_2(E_{\mathrm{F}})}. \tag{3}$$

Equation (2) results in a hard gap (no imaginary component of $\Delta_{1,2}$) for $E < E_{\mathrm{c}}$ when $\Delta_{1,2}$ are both larger than zero [62]. Here, E_{c} is a critical energy whose value depends on these parameters. As we are looking for pair breaking that resembles the spectral shape of Eq. (1) which does not have a hard gap, we are interested in the situation where $\Delta_2 = 0$. This is achieved when $\Delta_2^{\mathrm{BCS}} = 0$ and $\Gamma_{21} \ll \Gamma_{12}$. In the limit of vanishing Γ_{21}, Eq. (2) can be easily solved:

$$\begin{aligned} \Delta_1(E) &= \frac{\Delta_1^{\mathrm{BCS}} E}{E + i\Gamma_{12}}, \\ \Delta_2(E) &= 0. \end{aligned} \tag{4}$$

Inserting $\Delta_1(E)$ in Eq. (4) into the standard formula for the superconducting density of states exactly produces the Dynes formula with Γ_{12} equal to Γ (Ref. [39]). Therefore, interband scattering can cause the Dynes density of states when a nonsuperconducting band is present whose $N(E_{\mathrm{F}})$ is much larger than the $N(E_{\mathrm{F}})$ of the superconducting band.

This scenario is possibly relevant for the LaAlO$_3$–SrTiO$_3$ interface superconductor. It is well established that electrical transport at the LaAlO$_3$–SrTiO$_3$ interface happens in multiple bands [63–65] and that the presence of multiple bands also affects the superconductivity [26,29,31,32,66]. No consensus has been reached, however, about which bands are superconducting and which band provides most of the pairing interaction. Some reports argue that the low-energy band hosts the superconducting state [31,66] and others argue that the high-energy band hosts the superconducting state [26,32]. The latter scenario provides the possibility of having a superconducting band with small $N(E_{\mathrm{F}})$ together with a nonsuperconducting band with large $N(E_{\mathrm{F}})$. This is because the low-energy band has large $N(E)$ for energies larger than the avoided level crossing [67]. This scenario where the band with the largest n is nonsuperconducting can also explain the small superfluid density of the superconductor [68]. We note that in this scenario it is not required that the low-energy band is nonsuperconducting. It is sufficient when its gap is smaller than the resolution of our experiment ($\sim$5 μeV). Because our tunneling experiments probe predominantly electrons with $3d_{xz,yz}$ orbital character [26], we do not observe the lowest-energy band. Therefore, we cannot experimentally verify whether this band is superconducting or not.

Because Γ depends directly on Γ_{12} in this scenario, the correlation between Γ_0, the temperature-independent part of Γ, and Γ_1, the temperature-dependent part of Γ, can be explained (Fig. 6). Under the assumption that the scattering matrices for both types of interband scattering do not depend on n, both Γ_0 and Γ_1 will change as a result of the phase space for scattering. The phase space depends on the $N_1(E_{\mathrm{F}})/N_2(E_{\mathrm{F}})$ ratio. Modifying n changes the $N_1(E_{\mathrm{F}})/N_2(E_{\mathrm{F}})$ ratio and therefore also Γ_0 and Γ_1 in the same manner, explaining the correlation between the parameters.

Finally, the multiband scenario discussed above can explain why larger values of Γ are observed in the LaAlO$_3$–SrTiO$_3$ electron system than those observed in doped SrTiO$_3$ [69,70] because in the latter superconductor the band with the largest $N(E_{\mathrm{F}})$ is superconducting [71].

V. CONCLUSION

We have analyzed the spectral density of states $N(E)$ of the LaAlO$_3$–SrTiO$_3$ interface in the superconducting state as a function of temperature and gate voltage. We found that $N(E)$ is well described by Eq. (1) at all values of T and V_{G}. Therefore, pair-breaking scattering (Dynes Γ) is required for an adequate description of the superconducting gap function. The data exclude inelastic electron scattering and magnetic scattering as the origin of the pair breaking. Our work points to either scattering in a superconductor with an unconventional order parameter or elastic scattering between a superconducting band with a small $N(E_{\mathrm{F}})$ and a band with a large $N(E_{\mathrm{F}})$ that is either nonsuperconducting or superconducting with a gap smaller than $\sim$5 μeV as the origin of the pair-breaking scattering in the LaAlO$_3$–SrTiO$_3$ interface superconductor.

Several questions remain. In what way is the increase of Γ with decreasing n related to the reduction of T_{c} in the region of the phase diagram where T_{gap} remains large? An increase in Γ leads to a reduction of the superconducting condensation energy [49]. Can this reduction become large enough to enable 2D fluctuations to destroy superconductivity while the gap remains? Another question concerns the generality of the results. Most superconductors in which a large value of Γ is observed are not multiband or exotic superconductors. Therefore, can intraband scattering result in a loss of superfluid density such that most of the electron system becomes effectively normal conducting and thereby intraband scattering causes pair breaking by itself?

[1] J. Bardeen, L. Cooper, and J. Schrieffer, Phys. Rev. **108**, 1175 (1957).

[2] R. C. Dynes, V. Narayanamurti, and J. P. Garno, Phys. Rev. Lett. **41**, 1509 (1978).

[3] B. Mitrovic and L. A. Rozema, J. Phys.: Condens. Matter **20**, 015215 (2007).

[4] D. Dentelski, A. Frydman, E. Shimshoni, and E. G. Dalla Torre, Phys. Rev. B **97**, 100503(R) (2018).

[5] A. E. White, R. C. Dynes, and J. P. Garno, Phys. Rev. B **33**, 3549(R) (1986).

[6] S. Bose, A. M. Garcia-Garcia, M. M. Ugeda, J. D. Urbina, C. H. Michaelis, I. Brihuega, and K. Kern, Nat. Mater. **9**, 550 (2010).

[7] D. Sherman, U. S. Pracht, B. Gorshunov, S. Poran, J. Jesudasan, M. Chand, P. Raychaudhuri, M. Swanson, N. Trivedi, A. Auerbach, M. Scheffler, A. Frydman, and M. Dressel, Nat. Phys. **11**, 188 (2015).

[8] P. Szabo, T. Samuely, V. Haskova, J. Kacmarcik, M. Zemlicka, M. Grajcar, J. G. Rodrigo, and P. Samuely, Phys. Rev. B **93**, 014505 (2016).

[9] W. W. Warren, R. E. Walstedt, G. F. Brennert, R. J. Cava, R. Tycko, R. F. Bell, and G. Dabbagh, Phys. Rev. Lett. **62**, 1193 (1989).

[10] H. Ding, T. Yokoya, J. Campuzano, T. Takahashi, M. Randeria, M. Norman, T. Mochiku, K. Kadowaki, and J. Giapintzakis, Nature (London) **382**, 51 (1996).

[11] B. Sacépé, C. Chapelier, T. I. Baturina, V. M. Vinokur, M. R. Baklanov, and M. Sanquer, Nat. Commun. **1**, 140 (2010).

[12] C. Richter, H. Boschker, W. Dietsche, E. Fillis-Tsirakis, R. Jany, F. Loder, L. Fitting Kourkoutis, D. A. Muller, J. R. Kirtley, C. W. Schneider, and J. Mannhart, Nature (London) **502**, 528 (2013).

[13] Y. Nakagawa, Y. Saito, T. Nojima, K. Inumaru, S. Yamanaka, Y. Kasahara, and Y. Iwasa, Phys. Rev. B **98**, 064512 (2018).

[14] A. Ohtomo and H. Y. Hwang, Nature (London) **427**, 423 (2004).

[15] N. Reyren, S. Thiel, A. D. Caviglia, L. F. Kourkoutis, G. Hammerl, C. Richter, C. W. Schneider, T. Kopp, A.-S. Ruetschi, D. Jaccard, M. Gabay, D. A. Muller, J.-M. Triscone, and J. Mannhart, Science **317**, 1196 (2007).

[16] A. D. Caviglia, S. Gariglio, N. Reyren, D. Jaccard, T. Schneider, M. Gabay, S. Thiel, G. Hammerl, J. Mannhart, and J. M. Triscone, Nature (London) **456**, 624 (2008).

[17] R. C. Dynes, J. P. Garno, G. B. Hertel, and T. P. Orlando, Phys. Rev. Lett. **53**, 2437 (1984).

[18] B. Sacépé, C. Chapelier, T. I. Baturina, V. M. Vinokur, M. R. Baklanov, and M. Sanquer, Phys. Rev. Lett. **101**, 157006 (2008).

[19] B. Sacépé, T. Dubouchet, C. Chapelier, M. Sanquer, M. Ovadia, D. Shahar, M. Feigel'man, and L. Ioffe, Nat. Phys. **7**, 239 (2011).

[20] D. Sherman, G. Kopnov, D. Shahar, and A. Frydman, Phys. Rev. Lett. **108**, 177006 (2012).

[21] N. Miyakawa, J. F. Zasadzinski, L. Ozyuzer, P. Guptasarma, D. G. Hinks, C. Kendziora, and K. E. Gray, Phys. Rev. Lett. **83**, 1018 (1999).

[22] T. J. Reber, N. C. Plumb, Y. Cao, Z. Sun, Q. Wang, K. McElroy, H. Iwasawa, M. Arita, J. S. Wen, Z. J. Xu, G. Gu, Y. Yoshida, H. Eisaki, Y. Aiura, and D. S. Dessau, Phys. Rev. B **87**, 060506(R) (2013).

[23] S. Reber, TJ amd Parham, N. Plumb, Y. Cao, H. Li, Z. Sun, Q. Wang, M. Iwasawa, M. Arita, J. Wen, Z. Xu, G. Gu, Y. Yoshida, H. Eisaki, G. Arnold, and D. Dessau, arXiv:1508.06252.

[24] J. Zasadzinski, M. Warren, and A. Denchfield, Tunneling Spectroscopy of Single Cu-O layer Cuprate Superconductors, in *Proc. of the APS March Meeting Abstracts*, abstract id. S41.011 (2017).

[25] V. Haskova, M. Kopcik, P. Szabo, T. Samuely, J. Kacmarcik, O. Onufriienko, M. Zemlicka, P. Neilinger, M. Grajcar, and P. Samuely, Appl. Surf. Sci. **461**, 143 (2018).

[26] H. Boschker, C. Richter, E. Fillis-Tsirakis, C. W. Schneider, and J. Mannhart, Sci. Rep. **5**, 12309 (2015).

[27] E. Fillis-Tsirakis, C. Richter, J. Mannhart, and H. Boschker, New J. Phys. **18**, 013046 (2016).

[28] L. Kuerten, C. Richter, N. Mohanta, T. Kopp, A. Kampf, J. Mannhart, and H. Boschker, Phys. Rev. B **96**, 014513 (2017).

[29] L. Kuerten, E. Fillis-Tsirakis, C. Richter, J. Mannhart, and H. Boschker, Phys. Rev. B **98**, 054509 (2018).

[30] B. Altshuler and A. Aronov, Solid State Commun. **30**, 115 (1979).

[31] A. Joshua, S. Pecker, J. Ruhman, E. Altman, and S. Ilani, Nat. Commun. **3**, 1129 (2012).

[32] E. Maniv, M. Ben Shalom, A. Ron, M. Mograbi, A. Palevski, M. Goldstein, and Y. Dagan, Nat. Commun. **6**, 8239 (2015).

[33] J. Falson, D. Maryenko, B. Friess, D. Zhang, Y. Kozuka, A. Tsukazaki, J. H. Smet, and M. Kawasaki, Nat. Phys. **11**, 347 (2015).

[34] J. P. Pekola, V. F. Maisi, S. Kafanov, N. Chekurov, A. Kemppinen, Y. A. Pashkin, O.-P. Saira, M. Möttönen, and J. S. Tsai, Phys. Rev. Lett. **105**, 026803 (2010).

[35] C. R. Ast, B. Jaeck, J. Senkpiel, M. Eltschka, M. Etzkorn, J. Ankerhold, and K. Kern, Nat. Commun. **7**, 13009 (2016).

[36] S. Skalski, O. Betbeder-Matibet, and P. R. Weiss, Phys. Rev. **136**, A1500 (1964).

[37] M. V. Feigel'man and M. A. Skvortsov, Phys. Rev. Lett. **109**, 147002 (2012).

[38] S. Kaplan, C. Chi, D. Langenberg, J. Chang, S. Jafarey, and D. Scalapino, Phys. Rev. B **14**, 4854 (1976).

[39] A. Mikhailovsky, S. Shulga, A. Karakozov, O. Dolgov, and E. Maksimov, Solid State Commun. **80**, 511 (1991).

[40] X. Lin, C. W. Rischau, L. Buchauer, A. Jaoui, B. Fauque, and K. Behnia, npj Quantum Mater. **2**, 41 (2017).

[41] M.-J. Jin, S. Y. Moon, J. Park, V. Modepalli, J. Jo, S.-I. Kim, H. C. Koo, B.-C. Min, H.-W. Lee, S.-H. Baek, and J.-W. Yoo, Nano Lett. **17**, 36 (2017).

[42] Because the normal-state scattering involves back-scattering whereas the pair-breaking scattering can also be due to forward scattering, Γ_N does not strictly need to be larger than Γ but it must at least be of similar magnitude.

[43] L. Yu, Acta. Phys. Sin. **21**, 75 (1965).

[44] H. Shiba, Prog. Theor. Phys. **40**, 435 (1968).

[45] A. I. Rusinov, ZhETF **56**, 2047 (1969) [Sov. Phys.–JETP **29**, 1101 (1969)].

[46] F. Herman and R. Hlubina, Phys. Rev. B **94**, 144508 (2016).

[47] F. Herman and R. Hlubina, Phys. Rev. B **95**, 094514 (2017).

[48] F. Herman and R. Hlubina, Phys. Rev. B **96**, 014509 (2017).

[49] F. Herman and R. Hlubina, Phys. Rev. B **97**, 014517 (2018).

[50] P. Wittlich, H. Boschker, T. Asaba, L. Li, H. M. L. Noad, C. A. Watson, K. A. Moler, D. Daraselia, D. Japaridze, A. Shengelaya, J. Wang, J. Xia, and J. Mannhart, Phys. Rev. Mater. **3**, 104418 (2019).

[51] J. Varignon, L. Vila, A. Barthélémy, and M. Bibes, Nat. Phys. **14**, 322 (2018).

[52] X. Lin, A. Gourgout, G. Bridoux, F. Jomard, A. Pourret, B. Fauqué, D. Aoki, and K. Behnia, Phys. Rev. B **90**, 140508(R) (2014).

[53] X. Lin, C. W. Rischau, C. J. van der Beek, B. Fauqué, and K. Behnia, Phys. Rev. B **92**, 174504 (2015).

[54] G. Cheng, M. Tomczyk, S. Lu, J. P. Veazey, M. Huang, P. Irvin, S. Ryu, H. Lee, C.-B. Eom, C. S. Hellberg, and J. Levy, Nature (London) **521**, 196 (2015).

[55] D. Stornaiuolo, D. Massarotti, R. Di Capua, P. Lucignano, G. P. Pepe, M. Salluzzo, and F. Tafuri, Phys. Rev. B **95**, 140502(R) (2017).

[56] G. Singh, A. Jouan, G. Herranz, M. Scigaj, F. Sanchez, L. Benfatto, S. Caprara, M. Grilli, G. Saiz, F. Couedo, C. Feuillet-Palme, J. Lesueur, and N. Bergeal, Nat. Mater. **18**, 948 (2019).

[57] M. Briggeman, M. Tomczyk, B. Tian, H. Lee, J.-W. Lee, Y. He, A. Tylan-Tyler, M. Huang, C.-B. Eom, D. Pekker, R. S. K. Mong, P. Irvin, and J. Levy, Science **367**, 769 (2020).

[58] A. D. Caviglia, M. Gabay, S. Gariglio, N. Reyren, C. Cancellieri, and J.-M. Triscone, Phys. Rev. Lett. **104**, 126803 (2010).

[59] A. A. Golubov and I. I. Mazin, Phys. Rev. B **55**, 15146 (1997).

[60] M. Thiemann, M. H. Beutel, M. Dressel, N. R. Lee-Hone, D. M. Broun, E. Fillis-Tsirakis, H. Boschker, J. Mannhart, and M. Scheffler, Phys. Rev. Lett. **120**, 237002 (2018).

[61] W. L. McMillan, Phys. Rev. **175**, 537 (1968).

[62] J. Senkpiel, C. Rubio-Verdú, M. Etzkorn, R. Drost, L. M. Schoop, S. Dambach, C. Padurariu, B. Kubala, J. Ankerhold, C. R. Ast, and K. Kern, Phys. Rev. B **100**, 014502 (2019).

[63] R. Pentcheva, M. Huijben, K. Otte, W. E. Pickett, J. E. Kleibeuker, J. Huijben, H. Boschker, D. Kockmann, W. Siemons, G. Koster, H. J. W. Zandvliet, G. Rijnders, D. H. A. Blank, H. Hilgenkamp, and A. Brinkman, Phys. Rev. Lett. **104**, 166804 (2010).

[64] G. Berner, M. Sing, H. Fujiwara, A. Yasui, Y. Saitoh, A. Yamasaki, Y. Nishitani, A. Sekiyama, N. Pavlenko, T. Kopp, C. Richter, J. Mannhart, S. Suga, and R. Claessen, Phys. Rev. Lett. **110**, 247601 (2013).

[65] A. E. M. Smink, J. C. de Boer, M. P. Stehno, A. Brinkman, W. G. van der Wiel, and H. Hilgenkamp, Phys. Rev. Lett. **118**, 106401 (2017).

[66] A. E. M. Smink, M. P. Stehno, J. C. de Boer, A. Brinkman, W. G. van der Wiel, and H. Hilgenkamp, Phys. Rev. B **97**, 245113 (2018).

[67] Z. Zhong, A. Tóth, and K. Held, Phys. Rev. B **87**, 161102(R) (2013).

[68] J. A. Bert, K. C. Nowack, B. Kalisky, H. Noad, J. R. Kirtley, C. Bell, H. K. Sato, M. Hosoda, Y. Hikita, H. Y. Hwang, and K. A. Moler, Phys. Rev. B **86**, 060503(R) (2012).

[69] A. G. Swartz, H. Inoue, T. A. Merz, Y. Hikita, S. Raghu, T. P. Devereaux, S. Johnston, and H. Y. Hwang, Proc. Natl. Acad. Sci. USA **115**, 1475 (2018).

[70] A. G. Swartz, A. K. C. Cheung, H. Yoon, Z. Chen, Y. Hikita, S. Raghu, and H. Y. Hwang, Phys. Rev. Lett. **121**, 167003 (2018).

[71] X. Lin, G. Bridoux, A. Gourgout, G. Seyfarth, S. Krämer, M. Nardone, B. Fauqué, and K. Behnia, Phys. Rev. Lett. **112**, 207002 (2014).